Critical Spacecraft-to-Earth Communications for Mars Exploration Rover (MER) Entry, Descent and Landing

William J. Hurd[1]
818-354-2748
William.J.Hurd@jpl.nasa.gov

Polly Estabrook[1]
818-354-2275
Polly.Estabrook@jpl.nasa.gov

Caroline S. Racho[1]
818-354-6481
Caroline.S.Racho@jpl.nasa.gov

Edgar H. Satorius[1]
818-354-5790
Edgar.H.Satorius@jpl.nasa.gov

Jet Propulsion Laboratory
4800 Oak Grove Drive
Pasadena, CA 91109

Abstract— For planetary lander missions, the most challenging phase of the spacecraft to ground communications is during the entry, descent, and landing (EDL). As each 2003 Mars Exploration Rover (MER) enters the Martian atmosphere, it slows dramatically. The extreme acceleration and jerk cause extreme Doppler dynamics on the X-band signal received on Earth. When the vehicle slows sufficiently, the parachute is deployed, causing almost a step in deceleration. After parachute deployment, the lander is lowered beneath the parachute on a bridle. The swinging motion of the lander imparts high Doppler dynamics on the signal and causes the received signal strength to vary widely, due to changing antenna pointing angles. All this time, the vehicle transmits important health and status information that is especially critical if the landing is not successful. Even using the largest Deep Space Network antennas, the weak signal and high dynamics render it impossible to conduct reliable phase coherent communications. Therefore, a specialized form of frequency-shift-keying will be used. This paper describes the EDL scenario, the signal conditions, the methods used to detect and frequency-track the carrier and to detect the data modulation, and the resulting performance estimates.

TABLE OF CONTENTS

1. INTRODUCTION

Two Mars rover missions will be launched by NASA in May and June of 2003, during the 2003 Mars launch opportunity. They are the Mars Exploration Rovers, MERA and MERB. The spacecrafts will enter the Mars atmosphere directly, without first going into Mars orbit. The rovers will land on the Mars surface in January and February of 2004, in a similar manner to the successful Mars Pathfinder landing in 1996.

During the Entry, Descent and Landing (EDL) phases, it is important to maintain communications from the spacecraft to the Earth. Although this communication cannot affect the landing because the long round-trip-light time precludes real time feedback from Earth to the spacecraft, the communication could be critical to the success of future missions. This is especially true in case of a mission failure, when the diagnostic data would be very important.

Communication during EDL is very challenging, due to numerous factors. The EDL scenario and the factors limiting communications are discussed in Section 2. The communication signal set and the signal detection and tracking techniques are discussed in Section 3. Analysis and simulation performance estimates are presented in Section 4, SNR thresholds and detection strategy are discussed in Section 6, and a summary is given in Section 5.

2. MARS EDL SCENARIO

The EDL scenario for MERB is shown in Figure 1. The scenario for MERA is similar. The rover vehicle is enclosed

[1] 0-7803-7231-X/01/$10.00/© 2002 IEEE

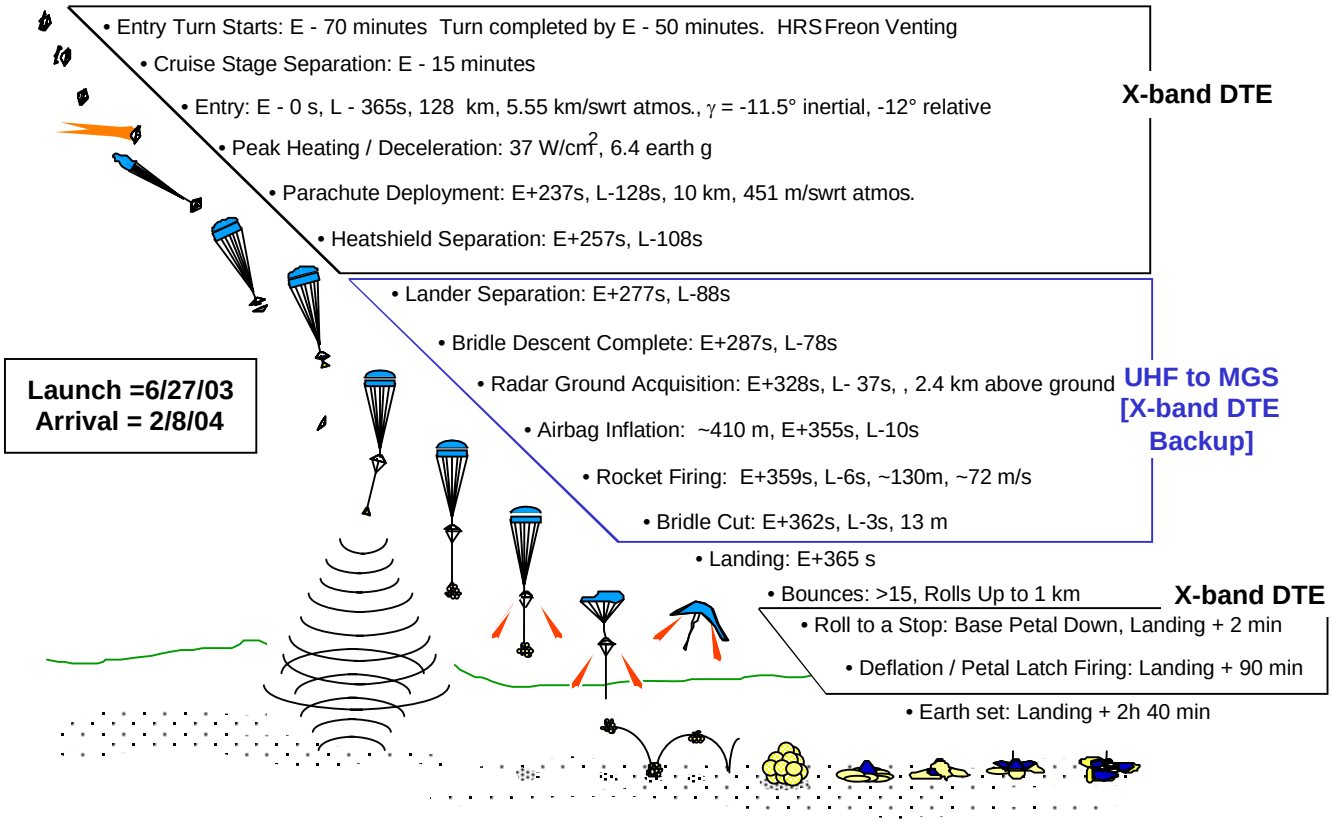

Figure 1. MERB EDL Nominal Sequence.

in a four-sided structure, shaped like a quadrahedron, called the lander. One triangular side is the base, and the other four sides are called petals. After landing, the petals are opened from the base and remain attached to the base. The rover is driven off the lander to conduct its operations.

EDL Sequence of Events

As the EDL scenario of Figure 1 begins, the lander is enclosed in a heatshield and a backshell, all attached to the main spacecraft. The entry turn begins approximately 70-min before entry, properly orienting the heat shield. When this is completed, approximately 15-min prior to entry, the cruise stage separation occurs, leaving the lander protected by the heat shield. Entry, defined as reaching a predefined altitude above the Mars surface, occurs approximately 365-s before landing.

During the hypersonic entry phase, the craft is rapidly slowed by the atmosphere. Approximately 237-s after entry, the craft has slowed sufficiently for the parachute to be deployed. Approximately 20-s later, the heatshield is released, and another 20-s later, or approximately 277-s after entry, the lander is separated from the backshell onto a bridle. The configuration then is the lander hanging from the backshell on the bridle, and the backshell hanging from the parachute.

For approximately 70 s, the lander swings back and forth on the bridle, and rotates on the order of 2 rpm due to the residual spin stabilization of the entire spacecraft. A radar on the lander is activated, and acquires a return signal from the Mars surface at approximately 328-s past entry, and 37-s before landing. An estimated 10-s prior to landing, using altitude information from the radar, the craft deploys airbags about the lander. About 4-s later, the retro rockets on the backshell are fired. When the rate of descent of the lander relative to the surface is close to zero, the bridle supporting the lander is cut, and the lander, encased in the airbags, falls freely to the surface. The lander bounces and rolls until it comes to a stop, after perhaps 2 min. The airbags are deflated within 90-min after landing. Earth set, ending the possible communication link to Earth, occurs approximately 2 h and 40 min after landing.

Communications Links

From cruise stage separation until the lander is separated from the backshell, communication is by a direct-to-Earth (DTE) X-band (8.4-GHz) link, using the backshell low-gain antenna (BLGA). After the lander separates from the backshell, the BLGA can no longer be used. From this point until landing, two methods of communication will be used: a DTE link using the rover low-gain antenna (RLGA), and a UHF relay link. The UHF link transmits the data to either the Mars Odyssey or the Mars Global Surveyor spacecraft,

which then relays the data to the Earth using a standard phase-coherent X-band link. The reason that the UHF relay link is used is that sufficiently reliable communication is not possible with the DTE link, as explained later. The UHF link is the prime communication link, but it is not as reliable as desired, so the DTE link will also be used, as a backup. Although the UHF link is prime during this period, it is not discussed further in this paper, because the subject of this paper is the DTE link. After landing, the UHF link will no longer be used, and the DTE link is again the only link.

The X-band DTE signal will be tracked by one of the three 70-m antennas of the NASA Deep Space Network (DSN). Which antenna(s) will be used is not yet known, because the landing sites for the two missions have not yet been chosen.

DTE Link Signal Format

The X-band DTE link will use a special multiple-frequency-shift-keyed (MFSK) signal format. This has been chosen because the signal conditions of high dynamics and low signal-to-noise ratio (SNR) will not reliably support phase coherent communications. There will be 256 different signal frequencies, modulated one at a time onto a residual carrier, using the spacecraft capability to switch the subcarrier frequency. During hypersonic entry, the signal frequency will be switched every 10 s, resulting in communication of 8 bits of information each 10 s. When the lander is suspended from the bridle, and the UHF link is prime, the duration of the modulation frequencies may be extended to 20 s, to better facilitate detection during this period of highly varying SNR. This would result in fewer messages of higher reliability than using the 10-s duration.

Dynamics

The expected MERB dynamics profile, magnitude and uncertainty are illustrated in Figure 2. The profiles are shown for one of the candidate landing sites. Three different profiles are shown, in green for the nominal entry path angle, and in red and blue for other path angles that correspond to the estimated maximum deviations from the nominal profile. For each entry angle, the spacecraft to Earth Doppler shift at the X-band frequency is shown in Figure 2a. The range of Doppler shift is approximately 90 kHz, and the (two-sided) range of Doppler uncertainty is approximately 50 kHz.

Figure 2b shows the Doppler rate, or first derivative of Doppler frequency, due to acceleration. The first maximum occurs due to atmospheric drag during hypersonic entry, at 150-s to 220-s past entry. The maximum varies from 700 Hz/s to 1200 Hz/s, depending on entry angle. The second maximum is a spike in Doppler rate due to parachute deployment. During the hypersonic entry, the range of uncertainty in Doppler rate is roughly the same as the

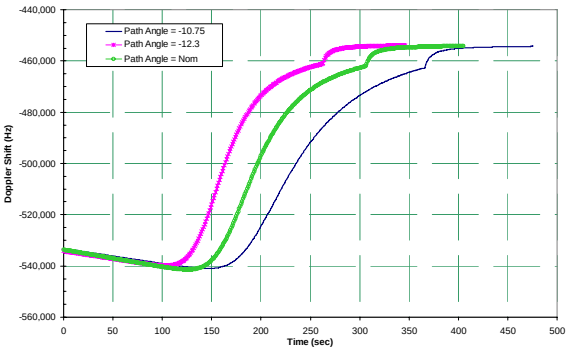

a. Doppler Frequency

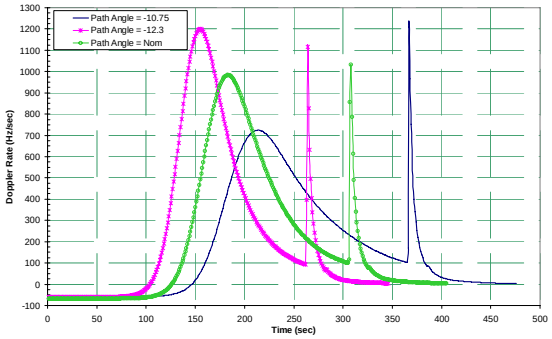

b. Doppler Frequency Rate

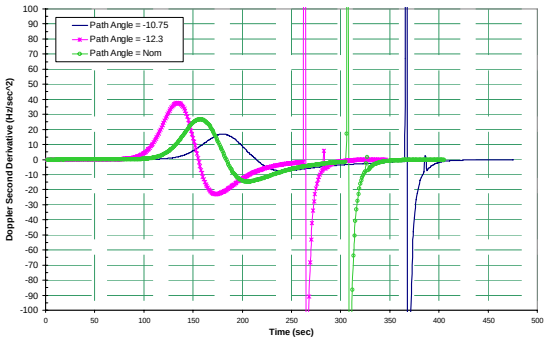

c. Doppler Second Derivative

Figure 2. Doppler Dynamics Profiles during EDL for Nominal, Maximum and Minimum Flight Path Angles

maximum possible Doppler rate. For example, at approximately 150-s past entry, the acceleration could be from approximately 0 Hz/s to 1200 Hz/s. The same is more obviously true for the parachute release.

Figure 2c shows the second derivative of Doppler frequency, due to jerk. During hypersonic entry, the value ranges from approximately -25 Hz/s^2 to 40 Hz/s^2. The exact values shown at parachute deployment are not meaningful due to the inaccuracy in the numerical differentiation used to obtain them. Most important is that modeling does not help to improve knowledge of this derivative, and could actually increase the error.

Signal-to-Noise Ratio

The SNR of the MERB downlink signal during EDL is shown in Figure 3. The SNR shown is the ratio of total received power to noise spectral density of the X-band signal received at a 70-m DSN antenna. These are the largest antennas available.

The total power received at the Earth from the spacecraft depends on the angle of the spacecraft with respect to the Earth and on the antenna gain pattern. The antenna gain depends both on the angle off the axis of rotation of the spacecraft, and on the rotation angle. The red (center) curve in Figure 3 is the nominal expected total power SNR versus time. This nominal SNR is based on the spacecraft axis orientation being the nominal angle, and on the nominal antenna gain with respect to rotation angle. The green (upper) curve is the maximum SNR that might be achieved, and is based on the most favorable orientation angle, and the blue (lower) curve is the minimum expected SNR. The three vertical dashed lines indicate the nominal times of the key events of parachute deployment at 246-s past entry, lander separation from the backshell at 276-s past entry, and full extension of the bridle with the lander at its end at 286-s past entry.

The backshell LGA (BLGA) is used from entry until lander separation. Throughout this time, the minimum expected SNR is 22 dB-Hz. It is 1-dB to 2-dB higher just before and

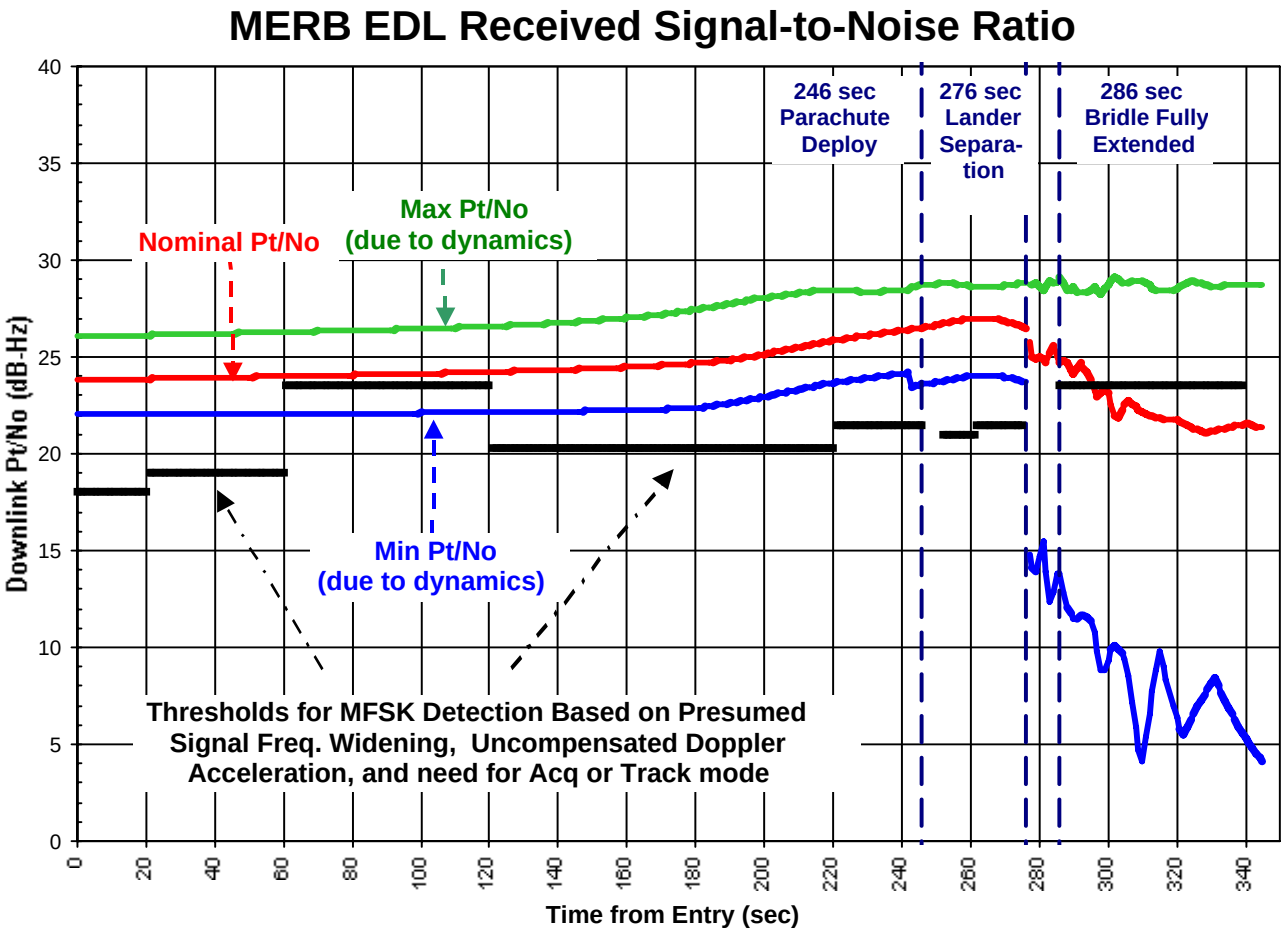

Figure 3. Signal to Noise Ratio During EDL

just after parachute deployment. When the lander is separated from the backshell, the BLGA can no longer be used, and the rover LGA (RLGA) is used for the DTE link. The pattern of this antenna is different from that of the BLGA. Also, beginning at this separation, the orientation of the antenna with respect to the Earth becomes further off the peak gain of the antenna, and becomes highly time varying and uncertain. One cause of this is that the attachment point of the bridle to the lander is offset from the spin axis by 15.7 deg, causing the antenna pattern to be offset from the direction to the backshell. Second, the rotational angle of the lander is unknown, and is changing on the order of 2 rpm due to the spin stabilization of the spacecraft. Finally, the lander will be swinging at the end of the bridle, due to the effects of the entry and due to unknown Martian wind. As a result of these effects, the SNR of the signal at the 70-m antenna can be anywhere from 5 dB-Hz to almost 30 dB-Hz. Furthermore, it is expected to vary widely within this range as the lander swings and rotates.

The UHF relay link was chosen as the prime link from lander separation to landing because the link margin is higher than for the DTE link, and because the UHF antenna has a different pattern than the RLGA, so that UHF link performance is affected less by spacecraft orientation.
The black horizontal line segments in Figure 3 show the estimated SNR threshold for the various portions of the EDL, when using the detection algorithms of this paper. This is discussed in Section 5.

Tracking and Detection Overview

During the highest dynamics, the combination of low SNR and high dynamics makes reliable phase-coherent communications impossible. For example, use of a type III phase locked loop (PLL) to track the dynamics would require a loop bandwidth on the order of 13 Hz. The required loop SNR should be approximately 11 dB, which is slightly higher than the 10-dB minimum for coherent communications when there is negligible dynamic phase lag error. With the 13-Hz loop bandwidth, this results in a required carrier-power-to-noise-density SNR of 22 dB-Hz. For the lowest SNR profile in Figure 3, the total power SNR is typically 22 dB-Hz. With half of the total power in the carrier, the carrier SNR would be 3-dB less than the nominal requirement. Furthermore, a PLL system would have virtually no chance to maintain lock during parachute deployment, and there would not be sufficient time to reacquire lock after deployment, in order to receive the important information sent then. There also would be no margin for lower SNR conditions, which are statistically possible. Thus coherent communication is not feasible.

Because coherent communication is not feasible, a special form of MFSK will be used, as described in Section 3. A major result of this paper is to demonstrate a method of frequency tracking that will perform satisfactorily throughout the hypersonic entry. It is shown that the SNR tracking threshold for this method is approximately 6-dB better than for a PLL.

For the Mars Pathfinder mission, there was a complete signal outage for approximately 30 s during the period of highest dynamics [1]. The cause of this signal loss is not known for sure. It may have been due to plasma outage, spectral spreading caused by vibration of the crystal oscillator in the transponder, or separation of electrical connections in the microwave system caused by excessive vehicle vibration. Regardless of the cause, this event may happen again for the MER missions. The frequency tracking method is amenable to recovering the signal after loss. The processing will be done non-causally, with recorded data. If the signal is lost, the plan is to reacquire it during the period of low dynamics shortly before parachute deployment. The tracking algorithm will then be applied backwards in time, recovering the data back to the end of the signal outage.

It is anticipated that lock will be lost upon parachute deployment. The signal will be reacquired shortly thereafter, and processed backwards in time to recover as much data as possible.

The final part of the scenario is after the lander is released from the backshell, and is suspended on the bridle. The lander is swinging in the wind, and rotating due to the spin stabilization of the spacecraft. This causes the antenna gain in the Earth direction to be low, rapidly varying and poorly predictable, resulting in low and widely varying SNR.

During this phase, the UHF relay link is prime, but the X-band DTE data will be processed as best as possible, as a backup. The X-band SNR is expected to vary over a range on the order of 20 dB. There will also be high unmodeled dynamics, due to the swinging and rotation of the lander. It is not expected that frequency tracking will be possible. Non-coherent detection algorithms will be used to search over the range of possible Doppler profiles. It is expected that signal detection will be successful when the SNR is at the higher end of its range. It is expected that some but not all of the FSK tones will be detected during this phase. Note that this phase lasts for approximately 80 s, so that there will be only four to eight distinct signals, depending on whether 20-s or 10-s duration tones are transmitted.

3. SIGNAL SET, DETECTION AND TRACKING

To facilitate the DTE X-band link, a special form of MFSK is used that comprises both a fixed frequency carrier and a square-wave subcarrier. This special MFSK signal format used for EDL is represented by:

$$s(t) = \cos\left\{2\pi \cdot f_c^{\,0} t + \Delta \cdot Sqr\left(2\pi \int_{-\infty}^{t} d\tau \cdot f_d(\tau)\right)\right\},$$

where f_c^0 is the transmitted carrier frequency; Δ is the modulation index ($\cos^2\Delta$ represents the fraction of the total power in the carrier); f_d denotes the data tone (1 of 256 possible tones transmitted every 10 s) and $Sqr(\cdot)$ is the hard-limited sine function:

$$Sqr(x) = \begin{cases} 1, 0 < x \le \pi \\ -1, \pi < x \le 2\pi \end{cases}$$
$$Sqr(x) = Sqr(x + 2\pi).$$

Spectrally, $s(t)$ comprises discrete lines at the carrier, data tone sidebands (on either side of the carrier line) and harmonics of the data tone created by the hard limiting function, $Sqr(\cdot)$.

The effect of the DTE channel is to introduce significant time-varying amplitude and Doppler (assumed to equally shift the carrier and data subcarrier tones) and to add noise. Thus, we can represent the received signal as:

$$x(t) = A(t)\cdot\cos\left\{2\pi\int_{-\infty}^{t} d\tau\cdot f_c(\tau) + \Delta\cdot Sqr\left(2\pi\int_{-\infty}^{t} d\tau\cdot f_d(\tau)\right)\right\} + n(t),$$

where the received carrier frequency can be represented as the sum of the transmitted frequency and a time varying Doppler component $\Delta f(t)$, i.e., $f_c(t) = f_c^0 + \Delta f(t)$.

In detecting and demodulating this waveform, the carrier frequency, $f_c(t)$, and its time derivative $\dot{f}_c(t)$ (frequency rate) are first tracked out via a Fast Fourier Transform (FFT)-based maximum likelihood detection approach [2]. The transmitted MFSK data tones are then determined. The process is depicted in Figure 4.

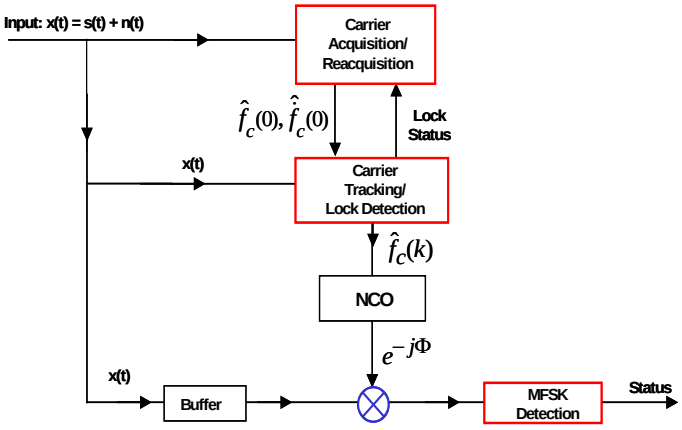

Figure 4. EDL demodulator.

The carrier acquisition process is essentially an open loop search over carrier frequency and rate space wherein different hypothesized rates are first mixed out of a segment of the input data, i.e.,

$$r_\ell(t) \equiv x(t)\cdot\exp\{-2\pi j(\hat{\dot{f}}_c^{\ell}(t)\cdot t^2/2)\},$$
$$0 \le t \le T; 1 \le \ell \le N_r,$$

where $\hat{\dot{f}}_c^{\ell}(t)$ denotes the $\ell - th$ hypothesized carrier frequency rate (N_r possible rates) and T is the time span of the segment. Each segment $r_\ell(t)$ is then sub-divided into M contiguous sub segments of duration $\Delta T = T/M$. FFTs of each sub segment are then computed and the magnitude-squared FFTs for each ℓ are averaged together to form the periodogram estimates $P_\ell(f)$, $1 \le \ell \le N_r$. Initial estimates of the carrier frequency and rate are then derived via:

$$\left.\begin{matrix}\hat{f} \\ \hat{\dot{f}}_\ell\end{matrix}\right\} = \arg\max_{\ell, f}\{P_\ell(f)\}$$

The resulting estimates, $\hat{f}_c(0) \equiv \hat{f}$ and $\hat{\dot{f}}_c(0) \equiv \hat{\dot{f}}_\ell$, are then used to initialize carrier frequency tracking. This is similar to the acquisition process except that carrier frequency and rate estimates derived from a T-length data segment are used as initial estimates for the next segment, and so on. For tracking, these segments are typically overlapped (50-75% overlapping) in order to provide smoother frequency estimates to the data tone demodulator and also to minimize large frequency excursions between estimates. In addition, the sizes of the frequency and frequency rate spaces are substantially reduced during tracking. Note that a lock detector can be used to monitor tracking performance and indicate if re-acquisition is required at any point in time.

The carrier acquisition/tracking parameters, T and ΔT, are chosen based on the anticipated dynamics. Specifically, since only the received carrier frequency and its first derivative are estimated directly, the presence of the second and higher order derivatives of frequency can degrade acquisition and tracking performance. To avoid these degradations, we choose ΔT sufficiently short that the maximum deviation of the received carrier frequency from a linear trajectory over the T-length segment is less than one-quarter of the FFT resolution, $\Delta f = 1/\Delta T$. Consequently, for a given Δf we choose $T = \sqrt{2\cdot\Delta f / \ddot{f}_{\max}}$, where $\ddot{f}_{\max}$ represents the maximum anticipated Doppler acceleration. In addition, Δf must be large enough to accommodate any spectral spreading induced, e.g., by vibration effects.

4. PERFORMANCE ESTIMATES

In deriving receiver performance estimates, we note that regardless of whether we are performing carrier acquisition, tracking or MFSK tone detection, the estimation process is always based on peak power detection. In the case of carrier acquisition, the maximum over all possible frequencies and rates is determined as the initial estimate of the carrier frequency. We denote the size of the search space (number of Doppler and Doppler rate pairs) by N_f and assume that the correct carrier signal is present in only 1 of the N_f search locations.

From a performance analysis standpoint, carrier tracking is considered to be the same as acquisition except that the size of the search space is drastically reduced and thus the tracking threshold is usually somewhat lower (~ 1-2 dB lower) than for acquisition. Likewise, MFSK tone detection is based on peak power estimation except that Doppler rate is eliminated from the search space and furthermore the number of frequencies searched is reduced to the possible MKSK tones.

Assuming chi-square statistics for the signal and noise periodogram data $P_\ell(f)$, the probability of correct carrier frequency identification is given by:

$$P_{id} = \int_0^\infty dx \cdot \{F_n(x)\}^{Nf-1} \cdot \left(\frac{x}{T \cdot CNR}\right)^{(M-1)/2} \cdot e^{-(x+T\cdot CNR)} \cdot I_{M-1}(\sqrt{4 \cdot x \cdot T \cdot CNR}),$$

where $I_{M-1}(\cdot)$ denotes the modified Bessel function of order $M-1$ ($M = T\Delta f$); $F_n(x)$ is the noise distribution, i.e., $F_n(x) = df_n(x)/dx$ and $f_n(x)$ is the noise probability density function: $f_n(x) = (x^{m-1}/(M-1)!) \cdot e^{-x}$. Also in the above expression for P_{id}, CNR is the carrier power-to-noise density ratio (recall that the ratio of carrier power to the total power is $\cos^2\Delta$).

Based on the above, we can compute carrier acquisition or tracking probabilities, e.g., versus the total received signal power (carrier plus data)-to-noise density ratio, $P_T/N_0 = CNR/\cos^2\Delta$. Consider a high-dynamics, carrier acquisition scenario wherein the FFT resolution is set at $\Delta f = 20\,Hz$; the non-coherent FFT averaging duration is $T = 1\,\text{sec}$; the frequency search space is 25 kHz wide; the frequency rate search space is 2000 Hz/s wide (in steps of 5 Hz/s) and $\Delta = 48^\circ$. The corresponding probability of incorrect carrier acquisition ($1 - P_{id}$) is plotted in Figure 5 versus P_T/N_0. In addition, a plot of $1 - P_{id}$ versus P_T/N_0 is also presented corresponding to a carrier tracking scenario wherein the search space has been reduced from {25 kHz X 2000 Hz/s} down to {100 Hz X 15 Hz/s}. As is seen, the carrier acquisition threshold at $P_{id} = 0.999$ is approximately 2 dB greater than for carrier tracking.

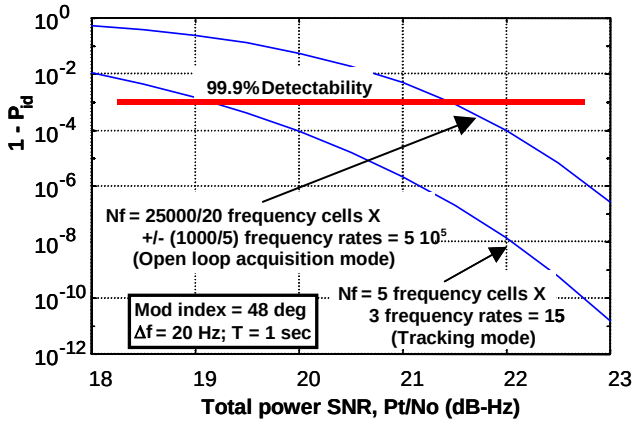

Figure 5. Probability of incorrect carrier acquisition/ tracking.

In the case of MFSK data tone detection, the probability of correct symbol detection is given by the above expression for P_{id} but with M replaced by $2M$ (due to spectral folding about the carrier prior to data tone detection) and with CNR replaced by the ratio of power in just one of the data tone sidebands to noise power spectral density. Also, for MFSK data tone detection and assuming perfect carrier tracking, N_f represents the number of possible tones transmitted (typically, $N_f = 256$) and the non-coherent integration time T is nominally matched to the data symbol duration but can be shorter with some loss in performance.

This is illustrated in Figure 6 where the MFSK symbol error probability is plotted versus P_T/N_0 (again assuming a 48 deg modulation index) corresponding to a $\Delta f = 1\,Hz$ FFT resolution and with both T = 5 s and 10 s non-coherent integration spans. Also in Figure 6, the number of possible transmitted tones is varied from 128 to 512 tones. As is seen, doubling T results in a 2-dB reduction in threshold at 0.001 symbol error probability. On the other hand, quadrupling the number of possible tones from 128 to 512 increases the threshold by only about 0.25 dB.

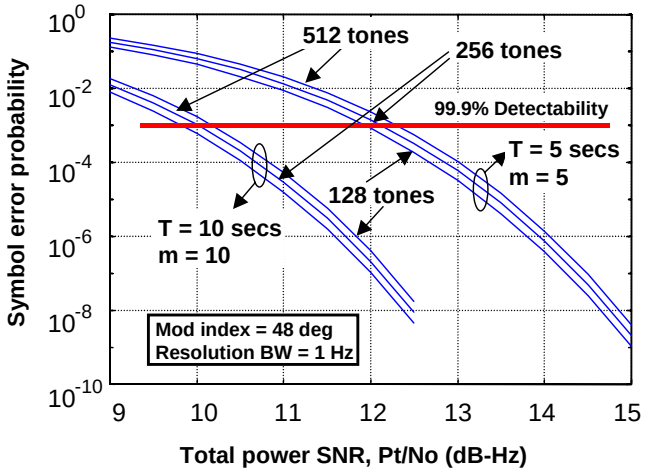

Figure 6. MFSK symbol error probability.

As an example of EDL tracking performance, we have simulated the MERB frequency profile (see Figure 2) and impressed it upon the transmitted carrier. Simulated tracking performance at 19.4 dB-Hz and Δ = 48 deg is presented in Figure 7. Utilizing a 10-Hz FFT resolution and a 0.7-s non-coherent integration time constant, we are able to continuously track the carrier through periods of peak dynamics all the way up to parachute deployment, occurring at approximately 240-s after entry (the track depicted in Figure 7 was terminated just prior to parachute deployment).

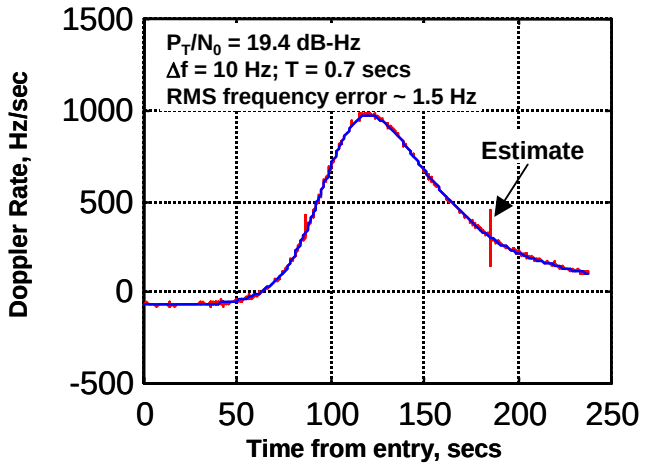

Figure 7. Simulated MERB EDL tracking.

Based on an analysis of carrier detectability as described above (Figure 5), we find that these detection parameters ($\Delta f = 10\,Hz$ and $T = 0.7$ sec) yield reliable stable tracking with mean time to lose lock on the order of 700 s at P_T / N_0 = 19.4 dB-Hz. This is confirmed by the simulation results depicted in Figure 7. Furthermore, based on the dynamic tracking considerations discussed above in Section 3, these detection parameters will avoid noticeable performance degradations for Doppler second derivatives as large as 40 Hz/s^2, which indeed corresponds to the peak value for MERB prior to parachute deployment (Figure 2).

It is noted that this performance far surpasses that of a PLL which requires a 22-dB-Hz CNR for reliable tracking under these conditions as discussed in Section 2. Given that $CNR = \cos^2 \Delta \cdot P_T / N_0 \approx 16\,dB - Hz$ for the simulated data presented in Figure 7, we see that the CNR tracking threshold for this method is at least 6-dB better than for a PLL. Note also from Figure 7 that the root-mean-square (RMS) frequency tracking error σ_f is approximately 1.5 Hz (in general $\sigma_f \propto \Delta f$). This is more than adequate for reliable MFSK tone detection as illustrated in Figure 8 where a waterfall display of the detected 10-s MFSK tones is depicted over time (approximately 23 tones transmitted from entry to parachute deployment). As is seen there is plenty of margin for correctly demodulating all of the data tones.

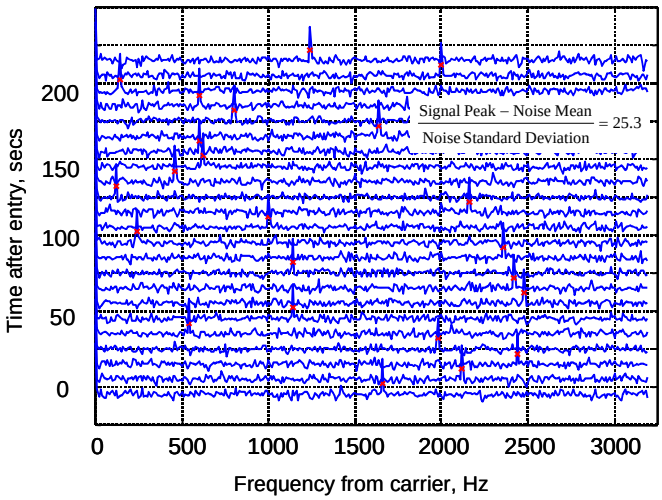

Figure 8 - Simulated MERB EDL tone detection.

The detected tones displayed in Figure 8 are generated by first mixing the carrier frequency estimate (Figure 7) from the simulated data (as depicted in Figure 4) and then performing MFSK tone detection. Given the excellent frequency stability of the tracker for this case (σ_f ~ 1.5 Hz), tone detection can be implemented with a much longer non-coherent integration time constant T than is used in tracking the carrier. In particular, T = 10 s is used for data tone detection in Figure 8 whereas T = 0.7 s for carrier tracking (Figure 7). In both cases a $\Delta f = 10\,Hz$ FFT resolution was implemented; however, a much smaller frequency resolution (on the order of σ_f) could be used for data tone detection if desired (depending on the extent of spectral spreading present).

5. Threshold and Detection Strategy

In Figure 3, the SNR threshold is shown for various phases of the EDL. The threshold depends mainly on the unmodeled dynamics, and are based on the preceding analysis, with 1.5 dB added for processing losses. During the portion of hypersonic entry with the highest dynamics, from 60-s to 120-s after entry, it is likely that there will be a total signal outage, as occurred for Pathfinder. The threshold shown has been increased by an additional 2.5 dB to account for the possible need for reacquisition. The resulting threshold shown for this time interval is 23.5 dB-Hz, compared to the 19.4 dB-Hz in the successful simulation results of Figure 7. The minimum expected SNR shown in Figure 3 is above the value of the successful simulation, but below the threshold shown. We conclude that successful tracking is likely but not certain, except during a total signal outage.

The system will record the received signal and apply the processing algorithms in non real time. This means that the data can be processed several times, using different values of FFT resolution, non-coherent detection time, and other parameters. The tracking algorithm can also be run backwards in time, which will be helpful if lock is lost at some point and then reacquired. Both of these techniques will be used if initial tracking is not successful.

When the signal is from the lander suspended from the bridle, the threshold is high due to the dynamics of the swinging and rotating lander. Both the coherent and non-coherent integration times are short. The motion also causes the SNR to vary rapidly. It is not likely that it will be possible to track the carrier frequency throughout this period. The planned detection strategy is to search over the possible ranges of frequency and frequency rate. Information from any detections that are made will be used to reduce the search region for the as yet undetected signals. Various sets of coherent and non-coherent detection times will be used. When the carrier is detected, it is highly likely that the FSK tone will be detected. In this manner, it is expected that some but not all of the FSK tone messages will be successfully detected.

6. Summary

A special form of 256-tone MFSK modulation will be used to communicate from the MER spacecraft to Earth during the challenging EDL phase of the mission. The residual carrier component of the signal will be acquired and tracked using FFT-based algorithms. The algorithms detect the signal and estimate frequency and frequency rate by maximizing a detection function over these parameters. This technique enables frequency tracking at a SNR approximately 6-dB lower than would permit coherent tracking with a phase-locked loop, under the same dynamics conditions. After tracking the carrier frequency, the MFSK tones are detected using similar processing. It has been shown that the modulation scheme and processing algorithms will be capable of reliable communication to Earth throughout most of the EDL phase.

7. Acknowledgements

The authors acknowledge the contributions of many members of the Mars Exploration Rover team, and the legacy contributions of the Mars Pathfinder team.

The research described in this publication was carried out by the Jet Propulsion Laboratory, California Institute of Technology, Pasadena, California, under a contract with the National Aeronautics and Space Administration.

References

[1] G. E. Wood, S. W. Asmar, T. A. Rebold and R. A. Lee., "Mars Pathfinder Entry, Descent, and Landing Communications," *The Telecommunications and Data Acquisition Progress Report 42-131*, Jet Propulsion Laboratory, Pasadena, California, November 15, 1997. http://tmo.jpl.nasa.gov/tmo/progress_report/42-131/131I.pdf

[2] V. A. Vilnrotter, S. Hinedi and R. Kumar, "Frequency Estimation Techniques for High Dynamic Trajectories," IEEE Trans. AES, V. 25, No. 4, July 1989.

Polly Estabrook *is the lead telecom system engineer for the Mars Exploration Rover and is responsible for the performance of the MER Entry Descent and Landing telecommunications system. She is the group supervisor of the Advanced Communications Systems Concepts Group in the Communications Systems Research Section at JPL. She has worked at JPL since 1988 primarily on the design of deep space in-situ (lander to orbiter, sensor web) communications systems and mobile satellite personal communication systems. She has written over 30 technical papers and chaired numerous IEEE and AIAA conference sesssions. She received the B.A. in Engineering Physics from the University of California, Berkeley, and the M.S. and Ph.D. in Electrical Engineering from Stanford University, California.*

William J. Hurd *received a B.S.E.E. degree from Clarkson University, Potsdam, New York, in 1961, and the M.S.E.E. and Ph.D.E.E. degrees from the University of Southern California in 1963 and 1967. He is currently a system architect in the InterPlanetary Network and Information Systems Directorate of the Jet Propulsion Laboratory, California Institute of Technology, Pasadena, California. He has been employed at JPL since 1967, and was previously a Member of the Technical Staff at Hughes*

Aircraft Co., where he was also a Hughes Master's Fellow and a Hughes Doctoral Fellow.

Caroline Racho *received her B.A. in Applied Mathematics from the University of California at Berkeley in 1986. She received her M.S. in Electrical Engineering from the University of Southern California in 1992. She is currently at the Jet Propulsion Laboratory, Pasadena ,California where she is a system engineer in the Wireless Communications Group. Her current areas of interest are in digital signal processing and communication systems.*

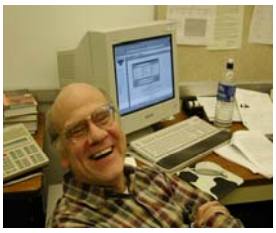

Edgar H. Satorius *is a senior member of the technical staff in the Communications Systems and Research Section of the Jet Propulsion Lab. He performs systems analysis in the development of digital signal processing and communications systems with specific applications to blind demodulation, digital direction finding and digital receivers. He has published over 90 articles and holds two patents in the field of digital signal processing and its applications. In addition, he is an Adjunct Associate Professor at the University of Southern California where he teaches digital signal processing courses. He received his B.Sc. in engineering from the University of California, Los Angeles and the M.S. and Ph.D. degrees in electrical engineering from the California Institute of Technology, Pasadena, California.*